



# Fano Resonance by Means of the One-Dimensional Superconductor Photonic Crystals

Arafa H. Aly<sup>1</sup> · Doaa Mohamed<sup>1</sup> · Hussein A. Elsayed<sup>1</sup> · Ahmed Mehaney<sup>1</sup>

Received: 2 March 2018 / Accepted: 21 March 2018 / Published online: 29 March 2018  
© Springer Science+Business Media, LLC, part of Springer Nature 2018

## Abstract

In the present work, we introduce a study about the reflectance properties of a one-dimensional superconductor photonic crystal in a different manner. Our structure is designed from alternately layers of high-temperature superconducting material (BSCCO) and a conventional superconducting material (Nb) terminated by the dielectric cap layer. The investigated numerical results are essentially based on the basics of the transfer matrix method and the two-fluid model. The numerical results showed the appearance of two sharp peaks, which are referred to Fano and electromagnetic-induced reflectance resonances. Also, we demonstrate the effects of many parameters on the reflectance properties of Fano resonance and the electromagnetic-induced reflectance. The effects of the constituent layer thicknesses, the number of periods, the operating temperature, the angle of incidence, and the refractive index of the dielectric cap layer are all considered. Finally, the effects of hydrostatic pressure on the Fano and EIR resonances are studied and calculated. This structure can play an important role in optical switching devices.

**Keywords** Fano resonance · EIR resonance · Superconductor photonic crystal · Transfer matrix method

## 1 Introduction

Photonic crystals (PCs) are periodic structures in one, two, and three dimensions [1]. These new composites opened a new covenant to optics due to their capability to control the propagation of electromagnetic waves [2, 3]. Such control can be investigated due to the appearance of some stop bands of specified frequencies in which the propagation of the incident electromagnetic waves of any frequency is effectively prohibited [4, 5]. These stop bands are named later the photonic band gaps (PBGs) [6–10]. Therefore, PCs become the cornerstone for many optical and medical applications such as filters, switches [11], modulators [12, 13], and biomedical sensors [14, 15]. Among the past decades, many types of materials such as dielectrics, organic, and dispersive materials are suggested in the design and fabrication of PCs. However,

PCs have a superconducting material in their components and are very interesting and promoted [16]. Such kind of PCs have the ability to control the width of the PBGs and provide tunable optical properties. Also, these materials possess the possibility for modifying its permittivity depending on its sensitivity to the external magnetic fields and the temperature [17]. In a different manner, the optical resonance phenomena have been appeared in PCs. PCs with such novelty could be used in many important applications such as narrowband optical filters [18], polarization selectors, modulators, switches, and sensors [19–21]. In recent years, a significant attention is devoted toward the Fano resonance and electromagnetic-induced reflectance (EIR) due to their symmetric line shape. Fano resonance is produced when a discrete quantum state interferes with a continuum band of states [22, 23]. Fano resonance phenomenon has received a considerable attention in the optical community due to their sharp transmission or reflection curves. These transmission curves could be promising in many optical and switching devices [24–26]. EIR is known as a sharp reflectance peak located in the middle of a broad resonance valley of the reflection curve. EIR is reported in planar materials [27] and coupling resonator waveguide [28, 29]. The physics of Fano

✉ Arafa H. Aly  
arafa.hussien@science.bsu.edu.eg

<sup>1</sup> Physics Department, Faculty of Science, Beni-Suef University, Beni-Suef, Egypt

resonance and EIR can be studied by the well-known model of two coupled driven oscillators [28–32].

In this article, we investigate theoretically both Fano and EIR line shapes in one-dimensional PCs. The theoretical modeling is essentially based on the two-fluid model and the transfer matrix method. Here, the one-dimensional PCs are designed using two different superconducting materials terminated by a dielectric cap layer. Also, the effects of several parameters on the line shape of Fano and EIR resonances such as the angle of incidence, the number of periods, the thicknesses of the constituent materials, the operating temperature of the superconducting materials, and the index of refraction of the cap layer are studied and discussed.

## 2 Theoretical Analysis

Figure 1 shows the schematic diagram of the one-dimensional superconductor PCs. This structure consists of two different superconducting materials, as shown in Fig. 1a, then we terminate it by adding a dielectric cap layer, as observed in Fig. 1b. The refractive index of the superconducting layer is frequency dependent and can be obtained based on the fundamentals of the two-fluid model [33–40]. Thus, the relative permittivity is given as:

$$\varepsilon_s(\omega) = 1 - \frac{c^2}{\omega^2 \lambda_L^2}. \quad (1)$$

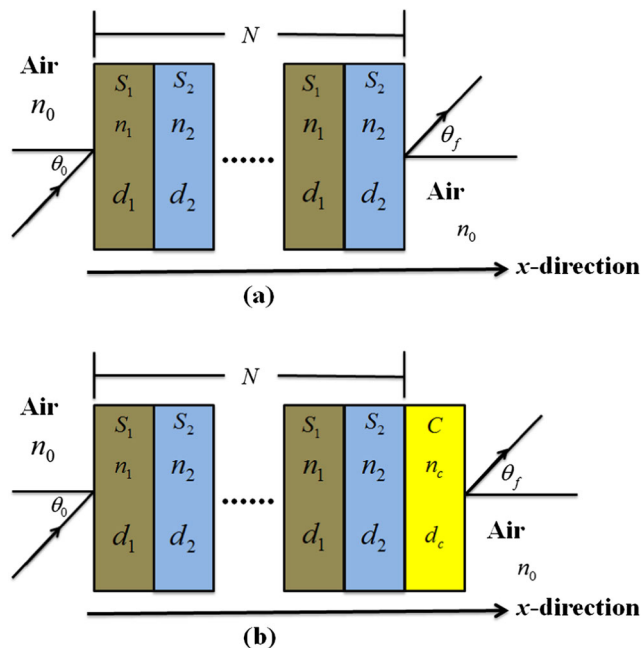


**Fig. 1** A schematic diagram of the proposed one-dimensional PC structure consists of two different superconductors  $S_1$  and  $S_2$  **a** without dielectric cap layer and **b** with the dielectric cap layer

where  $c$  is the velocity of light in a vacuum and  $\lambda_L$  is the London penetration depth that is given as:

$$\lambda_L = \lambda_L(T) = \lambda_0 / \sqrt{1 - (T/T_c)^q}, \quad (2)$$

where  $\lambda_0$  is the penetration depth at  $T = 0$  K,  $T$  is the operating temperature, and  $T_c$  is the critical temperature of the superconducting materials. Then,  $q = 2$  for high  $T_c$  superconducting materials and  $q = 4$  for low  $T_c$  superconducting materials. Therefore, the refractive index of the superconducting layer is equivalent to the square root of (1).

Using the two-fluid model and the transfer matrix method, the interaction between the incident electromagnetic waves and our design could be formulated. Such interaction can be obtained based on the analysis of the electric field interaction within the structure along the specified direction in terms of the dynamical and propagating matrices, thus we have [33–42]:

$$M = \begin{pmatrix} M_{11} & M_{12} \\ M_{21} & M_{22} \end{pmatrix} = D_0^{-1} (D_1 P_1 D_1^{-1} D_2 P_2 D_2^{-1})^N D_s, \quad (3)$$

where the dynamical matrices ( $D$ ) for TE waves are expressed as:

$$D_m = \begin{pmatrix} 1 & 1 \\ n_m \cos \theta_m & -n_m \cos \theta_m \end{pmatrix}, \quad (4)$$

with  $m = 0, 1$ , and 2. Whereas, the propagation matrices ( $P$ ) take the form:

$$P_m = \begin{pmatrix} \cos \phi_l + i \sin \phi_l & 0 \\ 0 & \cos \phi_l + i \sin \phi_l \end{pmatrix}, \quad (5)$$

where  $\phi_l = \frac{2\pi d_l}{\lambda} n_l \cos \theta_l$ ,  $l = 1$  and 2. Then, we can obtain the reflection coefficient using the matrix elements of (3) as follows:

$$r = \frac{M_{21}}{M_{11}}. \quad (6)$$

Finally, the reflectance for the incident wave is given as:

$$R = |r^2|. \quad (7)$$

## 3 Results and Discussion

In this section, we present the numerical results based on the aforementioned equations. Here, we demonstrate the variation of the reflectance properties of our structure with the normalized frequency at the normal incidence case. Our structure is designed from two different superconducting materials,  $S_1$ ,  $S_2$ , as observed in Fig. 1a. We consider the first layer to be Nb with ( $d_1 = 0.07 \mu\text{m}$ ,  $T_c = 9.25$  K,  $\lambda_0 = 0.0834 \mu\text{m}$ ) [41]. Wherein, the second one is BSCCO with ( $d_2 = 0.01 \mu\text{m}$ ,  $T_c = 95$  K,  $\lambda_0 = 0.15 \mu\text{m}$ ) [32]. Then,

we set the operating temperature to be  $T = 4.2$  K and the number of periods  $N = 50$ . The proposed structure is immersed in air. In the beginning, we demonstrate the effect of the cap layer on the reflectance characteristics of our structure. Then, we discuss the effect of the many parameters such as the angle of incidence, the number of periods, the thicknesses of the constituent materials, the operating temperature of the superconducting materials, and the cap layer index of refraction on the reflectance properties of our design. Figure 2 shows the variations of the reflectance versus the normalized frequency in the absence of the dielectric cap layer. The figure indicates the appearance of two symmetric narrow reflectance peaks ( $E$  and  $F$ ) with a narrow line width. The adjacent side bands of the two resonance peaks are close to zero.

In the presence of the dielectric cap layer with  $d_c = 20$  nm and  $n_c = 2.5$ , two important optical resonances appeared, as shown in Fig. 3. The figure shows that the dielectric cap layer has a significant effect in producing both the EIR and asymmetric Fano resonances. Moreover, the side bands around peak  $E$  form a broad upward reflectance valley which is known as the EIR resonance. In addition, the amplitude of peak  $E$  increases but the spectral position remains unchanged. The side bands of peak  $F$  form a broad downward concavity with a amplitude and with no change in the spectral position. This feature is useful for many applications, allowing the reflectance to be switched from total reflection to total transmission. So, it can underpin the concept of many switching devices in photonics.

Now, we discuss the effect of different parameters on the reflectance properties of our structure for TE waves. Firstly, Fig. 4 shows the effect of the angle of incidence on the characteristics of EIR and Fano resonance. At  $\theta = 0^\circ$ , Fano resonance and EIR are obtained at 1.11 and 1.56 normalized frequencies, respectively. As the angle of incidence increases to  $10^\circ$  and  $20^\circ$ , both Fano resonance

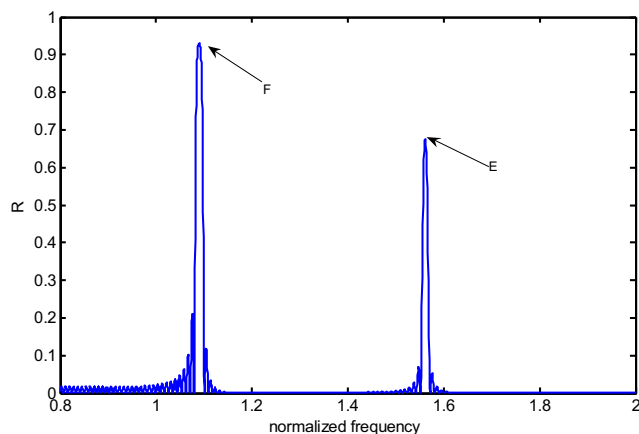


Fig. 2 Reflectance spectra of our periodic structure against the normalized frequency

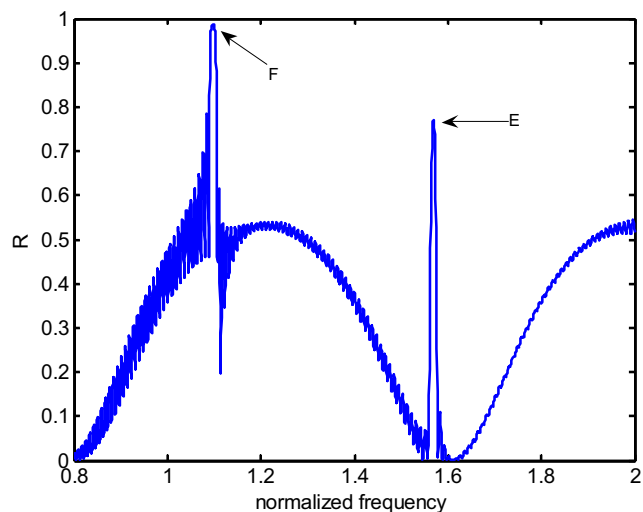


Fig. 3 Reflectance spectra of the one-dimensional superconductor PCs in the presence of the dielectric cap layer

and EIR are shifting toward the high frequencies. In addition, their amplitudes are almost unaffected. For further increment of  $\theta = 0^\circ$  to  $\theta = 30^\circ$  peaks shifting toward the higher frequencies are still present. However, the second peak (peak  $E$ ) begins to appear in an asymmetric line shape like the Fano resonance peak. The EIR turned to another shape of Fano resonance; this result is explained by the two coupled oscillator modes [28–30]. Two coupled oscillator modes describe EIR resonance as a special case of Fano resonance when the frequencies of strongly and weakly damped oscillators matched. As the incident angle increases to  $30^\circ$ , the phase shift changes and EIR turns to Fano

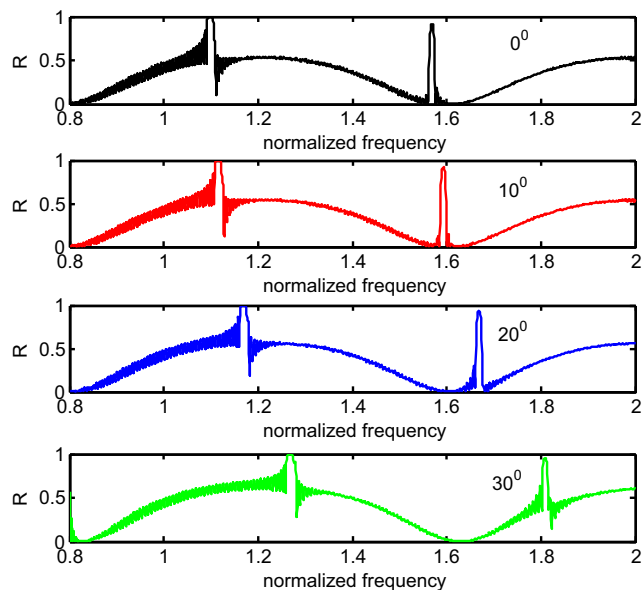
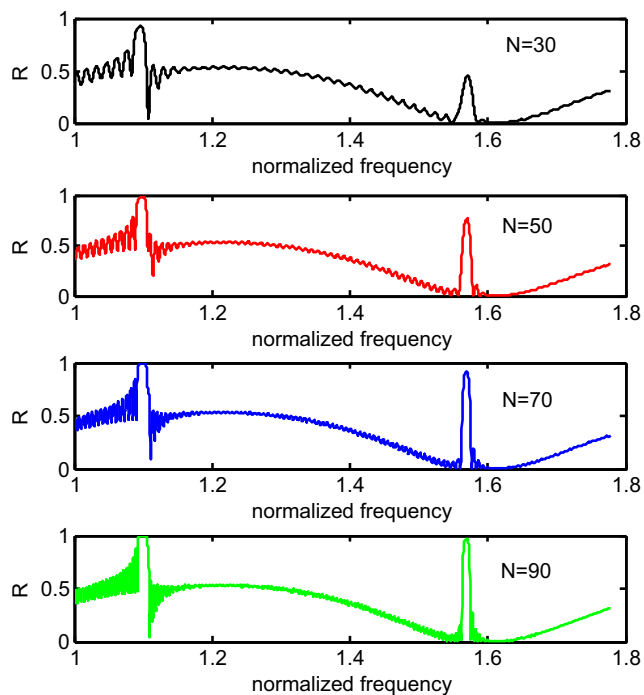


Fig. 4 The response of Fano resonance and EIR with the variation of the angle of incidence

resonance. Thus, the variation of the angle of incidence plays a distinct role in controlling the position of EIR and Fano resonances.

Secondly, we discuss the effect of the number of periods on the properties of Fano and EIR resonances, as shown in Fig. 5. Figure 5 shows that the number of periods has a significant effect on both EIR and Fano resonances. As the number of periods increases from 30 to 50, 70, and 90, Fano resonance line shape shows an abrupt change from high to low reflectance with a narrow line width. Furthermore, the difference between the maxima and minima in Fano resonance peak increases as well. On the other side, the reflectance values of the EIR resonance peak increases with the number of periods, as shown in the figure. Moreover, the width of this peak decreases with the increments of the number of periods. However, the positions of the EIR and Fano resonance are almost unaffected by the variation of the number of periods. Therefore, the number of periods plays an important role in controlling the reflectance properties of Fano and EIR resonance peaks.

Thirdly, Fig. 6 illustrates the effect of the refractive index of the dielectric cap layer on the EIR and Fano resonances. At  $n_c = 1.3$ , both Fano resonance and EIR peaks take symmetrical line shapes with high reflectance values close to unity. As the value of  $n_c$  increases from 1.3 to 1.6 and 2, the reflectance properties of Fano resonance peak are almost unchanged. However, the EIR peak begins to change from the symmetrical line shape to the asymmetrical line shape.



**Fig. 5** The effect of the number of periods on the reflectance characteristics of EIR and Fano resonance peaks

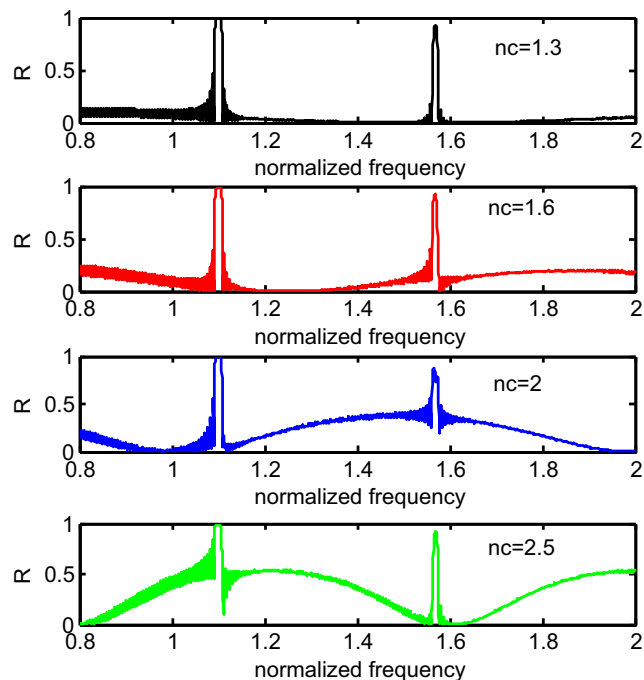
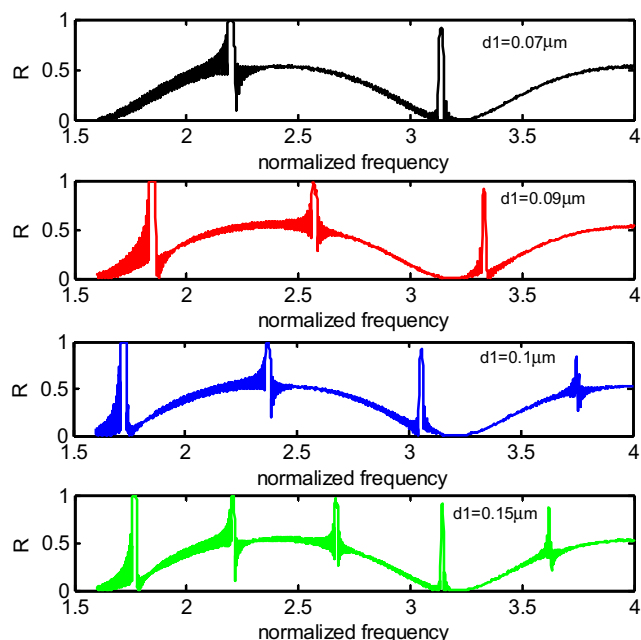


**Fig. 6** Reflectance spectra of our structure at different values of the refractive index of the dielectric cap layer

In addition, the maxima and the minima of this peak are strongly affected with the increase of  $n_c$  value, as shown in the figure. For  $n_c = 2.5$ , the EIR peak begins to return to the symmetrical line shape. Whereas, Fano resonance peak varies to the asymmetrical line shape. Such parameter could be crucial in adjusting the reflectance characteristics and the shape of Fano resonance and EIR peaks.

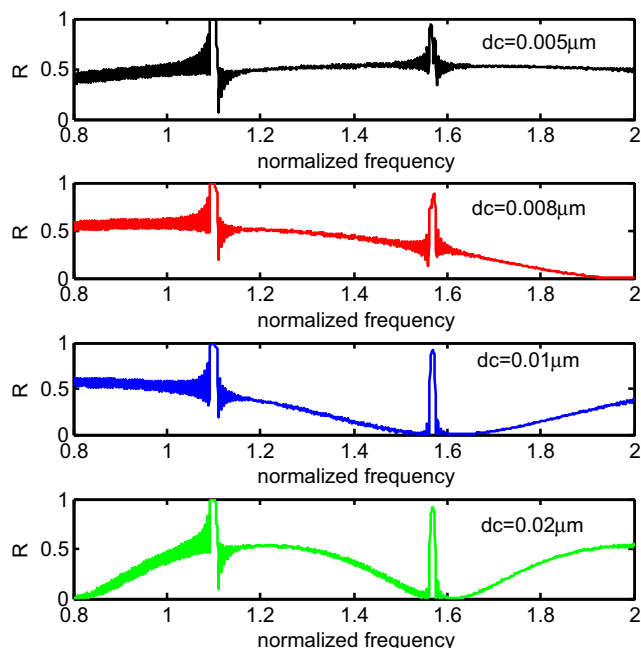
In what follows, we study the effect of the thickness variation of the first superconductor layer on the reflectance properties of our design. Figure 7 shows the distinct effect of  $d_1$  on Fano and EIR resonances. As  $d_1$  increases from 0.07 to 0.09  $\mu\text{m}$ , Fano resonance peak is shifted downwards the low-frequency regions with the appearance of a new Fano resonance peak at normalized frequency value equals to 2.6. Whereas, the EIR resonance peak shifted toward the high normalized frequency regions, as shown in the figure. Wherefore, the phase shift between the EIR and the first Fano resonance peaks increased. As  $d_1$  increases to 0.07 and 0.15  $\mu\text{m}$ , new Fano resonance peaks of asymmetrical and symmetrical line shapes begin to appear between the first Fano resonance and the EIR peaks. Moreover, the EIR resonance peak appeared in the asymmetrical line shape. Figure 7 demonstrates that the number of Fano resonance peaks could be controlled depending on the first superconducting layer thickness. Such property could play an important role in many optical switching devices.

Figure 8 shows the reflectance properties of EIR and Fano resonances at different thicknesses of the dielectric



**Fig. 7** Reflectance spectra of our structure at different values of the first superconductor layer thickness

cap layer ( $d_c = 0.005 \mu\text{m}$ ,  $d_c = 0.008 \mu\text{m}$ ,  $d_c = 0.01 \mu\text{m}$ ,  $d_c = 0.02 \mu\text{m}$ ). At  $d_c = 0.005 \mu\text{m}$ , there are two asymmetric resonance peaks in the reflectance spectrum corresponding to Fano and EIR resonances. As  $d_c$  increases to 0.008, 0.01, and 0.02  $\mu\text{m}$ , the position and the shape line of Fano resonance peak are almost unaffected. However, the position of the EIR has shifted downwards the low



**Fig. 8** The dependence of the position and the shape line of the EIR and Fano resonance peaks on the dielectric cap layer thickness

normalized frequency regions. Wherefore, the phase shift between Fano resonance and the EIR peaks decreases. In addition, the EIR peak line shape changes from the asymmetrical shape at  $d_c = 0.008 \mu\text{m}$  to the symmetrical shape at  $d_c = 0.01$  and  $0.02 \mu\text{m}$  as shown in the figure.

### 3.1 The Effects of the Operating Temperature on 1DSPC

In this section, we present the effects of the operating temperature on the reflectance properties of our design. Figure 9 shows that the operating temperature has a slight influence on the EIR and Fano resonance peaks. As the operating temperature ( $T$ ) varies from 2 to 4 K, the resonance peaks are shifted downwards the low normalized frequencies with a small decrease in the intensity of the EIR peak as observed in Fig. 9. For more increments in the value of the operating temperature, the intensity of the EIR peak decreases till reaches it 0.2 at  $T = 7$  K. in addition, Fano resonance peak becomes sharper.

### 3.2 The Effects of the Hydrostatic Pressure on 1DSPC

Finally, we studied the effects of hydrostatic pressure on the reflectance spectrum of 1DSPC ( $T = 4.2$  K and  $N = 50$  period) at the normal incidence case. The thickness of the first superconducting layer will be considered to  $d_1 = 75 \mu\text{m}$ . According to the compressibility constant  $k_a = 2.57 \times 10^{-3} \text{Gpa}^{-1}$ , the thickness of the superconducting layer can be modified as the reference [43, 44].  $\lambda_0$  is

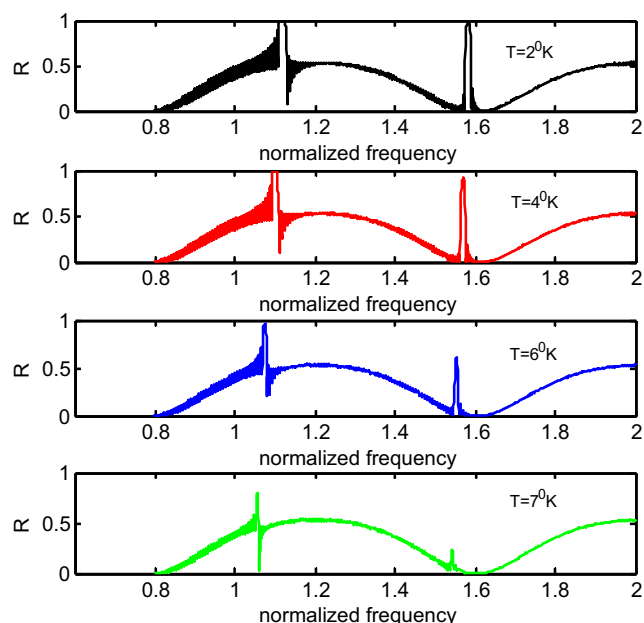


**Fig. 9** Variation of reflectance with normalized frequency at different values of the operating temperature

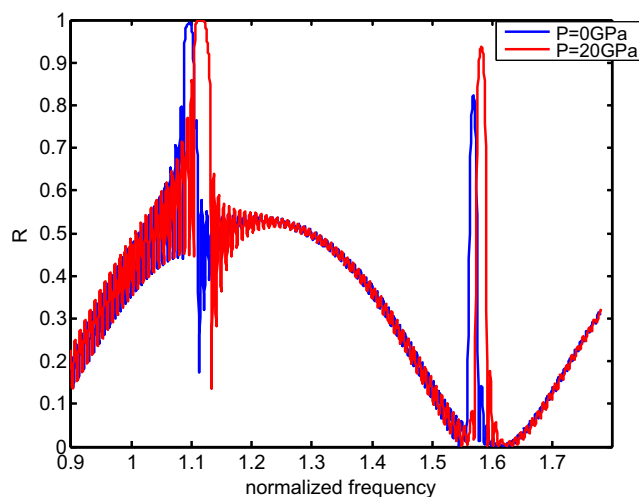
assumed to be constant, and the critical temperature of the superconducting layer due to the applied pressure can be described from the following relation  $T_c = q_1 + q_2 \times P + q_3 \times P^2$ , where  $q_1$ ,  $q_2$  and  $q_3$  are constants and we can calculate as similar in references [45, 46].

Figure 10 shows the reflectance spectrum as a function of the normalized frequency and hydrostatic pressure. By increasing the hydrostatic pressure from zero to 20 GPa, Fano resonance is shifted to the higher normalized frequency region with increasing the difference between its maximum and minimum peaks. Also, EIR resonance is shifted to the higher normalized frequency region with increasing its peak reflectance value. This variation can be explained according to the relations between the critical temperature and the applied pressure. By increasing the pressure value, the critical temperature increases and the fraction  $T/T_c$  become smaller which leads to the shift of EIR and Fano resonances to the high normalized frequency region. Moreover, we note that when we increase the hydrostatic pressure to more than 20 GPa, there is no change observed, which means EIR and Fano resonances are sensitive to the hydrostatic pressure till 20 GPa.

## 4 Summary and Conclusions

In summary, we can conclude our findings as follows:

1. Based on the fundamentals of the transfer matrix method, we investigated the reflectance properties of the one-dimensional superconductor PCs theoretically. Our periodic structure is designed from alternate layers of high-temperature superconducting material and conventional superconducting material terminated by the dielectric cap layer.



**Fig. 10** Reflectance spectrum of 1DSPC at two values of zero hydrostatic pressure  $P = 0$  and 20 GPa

2. The investigated results showed the appearance of two resonance peaks that correspond to Fano resonance and EIR. The presence of the dielectric cap layer has a significant role on the reflectance characteristics of the two resonance peaks.
3. The tunable features of Fano and EIR resonances can vary by different parameters. Since the angle of incidence, the number of periods, the thicknesses of the constituent materials, and the operating temperature could change the position, the line shape, the intensity, and the number of resonance peaks. These results show that the proposed structure could be suitable for many potential applications in optical switches and the sensing of Fano resonance line profile.
4. By studying the effect of hydrostatic pressure on the Fano and EIR resonances, it was found that Fano and EIR resonances can be shifted to the higher normalized frequency region with increasing the pressure value of the superconductor PCs structure.

## References

1. Yablonovitch, E.: Inhibited spontaneous emission in solid-state physics and electronics. *Phys. Rev. Lett.* **58**, 2059 (1987)
2. Asdi, R., Bagheri, S., Khaie, M., Malek, M., Tavassoly, M.T.: Tunable Fano resonance in large-scale polymer-dielectric slab photonic crystals. *Microelectron. Eng.* **97**, 201–103 (2012)
3. Athe, P., Srivastava, S., Thapa, K.B.: Electromagnetically induced reflectance and Fano resonance in one-dimensional superconducting photonic crystal. *Physica C: Supercond. Appl.* **547**, 36–40 (2018)
4. Joannopoulos, J.D., Johnson, S.G., Winn, J.N., Meade, R.D.: *Photonic Crystals: Molding the Flow of Light*. Princeton University Press (1995)
5. Aly, A.H.: Metallic and superconducting photonic crystal. *J. Supercond. Nov. Magn.* **21**, 421–425 (2008)
6. John, S.: Strong localization of photons in certain disordered dielectric superlattices. *Phys. Rev. Lett.* **58**, 2486 (1987)
7. Noda, S., Yamamoto, N., Imada, M., Kobayashi, I., Okano, M.: Alignment and stacking of semiconductor photonic bandgaps by wafer-fusion. *J. Lightwave Technol.* **17**, 1948 (1999)
8. Aly, A.H., Hsu, H.-T., Yang, T.-J., Wu, C.-J., Hwangbo, C.K.: Extraordinary optical properties of a superconducting periodic multilayer near zero permittivity operation range. *J. Appl. Phys.* **105**, 083917–6 (2009)
9. Aly, A.H., Sabra, W.: Effective surface impedance of a high-temperature superconductor. *Physica C: Supercond.* **495**, 126–129 (2013)
10. Aly, A.H., Elsayed, H.A., El-Naggar, S.A.: The properties of cutoff frequency in two-dimensional superconductor photonic crystals. *J. Modern Opt.* **61**(13), 1064–1068 (2014)
11. Hawkeye, M.M., Brett, M.J.: Narrow bandpass optical filters fabricated with one-dimensionally periodic inhomogeneous thin films. *J. Appl. Phys.* **100**, 044322 (2006)
12. Notomi, M., Shinya, A., Mitsugi, S., Kira, G., Kuramochi, E., Tanabe, T.: Optical bistable switching action of Si high-Q photonic-crystal nanocavities. *Opt. Express* **13**, 2678 (2005)
13. Hadfield, R.H.: Single-photon detectors for optical quantum information applications. *Nat. Photon.* **3**, 696 (2009)

14. Yokoyama, H.: Physics and device applications of optical microcavities. *Science* **256**, 66 (1992)
15. Vahala, K.J.: Optical microcavities. *Nature* **424**, 839 (2003)
16. Kuzmiak, V., Maradudin, A.A.: Photonic band structures of one- and two-dimensional periodic systems with metallic components in the presence of dissipation. *Phys. Rev. B* **55**, 7427 (1997)
17. Ooiet, C.H.R. et al.: Electromagnetic wave propagation through a high temperature superconductor-dielectric photonic crystal. *Phys. Rev. B* **61**, 5920 (2000)
18. Yu, Y., Heuck, M., Hu, H., Xue, W., Peucheret, C., Chen, Y., Oxenlowe, L.K., Yvind, K., Mork, J.: Fano resonance control in a photonic crystal structure and its application to ultrafast switching. *Appl. Phys. Lett.* **105**, 06117 (2014)
19. Bertoni, H.L., Cheo, L.H.S., Tamir, T.: Frequency selective reflection and transmission by aperiodic dielectric layer. *IEEE Trans. Antennas Propag.* **37**, 78–83 (1989)
20. Wang, S.S., Magnuson, R., Bagby, J.S., Moharam, M.G.: Guided-mode resonance in planar dielectric layer diffraction grating. *J. Opt. Soc.-Am.* **A7**, 1470–1474 (1990)
21. Magnuson, R., Wang, S.: New principle for optical filters. *Appl. Phys. Lett.* **61**, 1022–1024 (1992)
22. Limonov, M.F., Rybin, M.V., Poddubing, A.N., Kivshar, Y.S.: Fano resonance in photonics. *N. Photon*, 142 (2017)
23. Connerade, J.P., Lane, A.M.: Interacting resonance in atomic spectroscopy. *Rep. Prog. Phys.* **51**, 1439–1478 (1988)
24. Liu, N., Weiss, T., Mesch, M., Langguth, L., Eigenthaler, U., Hirscher, M., Sonnichsen, C., Giessen, H.: Planar metamaterial analogue of electromagnetically induced transparency for plasmonic sensing. *Nano Lett.* **10**, 1103 (2009)
25. Vafapour, Z.: Near-infrared biosensor based on classical electromagnetically induced reflectance (CI-EIR) in a planar complementary metamaterial. *Opt. Commun.* **387**, 1 (2017)
26. Yang, X., Yu, M., Kwong, D.L., Wong, C.W.: All optical analog to electromagnetically induced transparency in multiple coupled photonic crystal cavities. *Phys. Rev. Lett.* **102**, 173902 (2009)
27. Feng, D.C., Ting, Z.Y., Quan, Y.J., Ling, S.C., Gang, X.D., Zhong, Z.G.: Reflection-type electromagnetically induced transparency analog in terahertz metamaterials. *Chin. Phys. B* **23**, 124203 (2014)
28. Marangos, J.P.: Electromagnetically induced transparency. *J. Mod. Opt.* **45**, 471 (1998)
29. Verslegers, L., Yu, Z., Ruan, Z., Catrysse, P.B., Fan, S.: From electromagnetically induced transparency to superscattering with a single structure: A coupled-mode theory for doubly resonant structures. *Phys. Rev. Lett.* **108**, 083902 (2012)
30. Yang, Y., Kravchenko, I.I., Briggs, D.P., Valentine, J.: All dielectric metasurface analogue of electromagnetically induced transparency. *Nat. Commun.* **5**, 5753 (2014)
31. Joe, Y.S., Satanin, A.M., Kim, C.S.: Classical analogy of fano resonance. *Phys. Script* **74**, 259–266 (2006)
32. Khanikaev, A.B., Wu, C., Shvets, G.: Fano resonant metamaterials and their applications. *Nanophotonics* **2**(4), 247–264 (2013)
33. Khitrova, G., Gibbs, H.M., Kira, M., Koch, S.W., Scherer, A.: Vacuum Rabi splitting in semiconductors. *Nat. Phys.* **2**, 81 (2006)
34. Peng, B., Ozdemir, S.K., Chen, W., Nori, F., Yang, L.: What is and what is not electromagnetically induced transparency in whispering-gallery microcavities. *Nat. Commun.* **5**, 5082 (2014)
35. Aly, A.H., Mohamed, D.: BSCCO/SrTiO<sub>3</sub> one dimensional superconducting photonic crystal for many applications. *J. Supercond. Nov. Magn.* **18**, 1699–1703 (2015)
36. Aly, A.H., Aghajamali, A., Elsayed, H.A., Mobarak, M.: Analysis of cutoff frequency in a one-dimensional superconductor-metamaterial photonic crystal. *Phys. C* **528**, 5–8 (2016)
37. Aly, A.H., Sayed, W.: Superconductor-semiconductor metamaterial photonic crystals. *J. Supercond. Nov. Magn.* **29**, 1981–1986 (2016)
38. Aly, A.H., Mehaney, A., El-Naggar, S.: Evolution of phononic band gaps in one-dimensional phononic crystals that incorporate high- $T_c$  superconductor and magnetostrictive materials. *J. Supercond. Nov. Magn.* **30**, 2711–2716 (2017)
39. Elsayed, H.A., Aly, A.H.: Terahertz frequency superconductor-nanocomposite photonic band gap. *IJMPB* **32**(5), 1850056 (2018)
40. Aly, A.H. et al.: Optical properties of new type of superconductor-semiconductor metamaterial photonic crystals. *J. Supercond. Nov. Magn.* (2018). <https://doi.org/10.1007/s10948-018-4628-5>
41. Yeh, P.: *Optical Wave and Layered Media*. Wiley, Singapore (1991)
42. Tinkham, M.: *Introduction to Superconductivity*, 2nd edn. McGraw-Hill, New York (1996)
43. Yamamoto, A., Takeshita, N., Terakura, C., Tokura, Y.: *Nat. Commun.* **6**, 8990 (2015)
44. Takeshita, N., Yamamoto, A., Iyo, A., Eisaki, H.: *J. Phys. Soc. Jpn.* **82**, 023711 (2013)
45. Hunter, B.A., Jorgensen, J.D., Wagner, J.L., Radaelli, P.G., Hinks, D.G., Shaked, H., Hitterman, R.L.: *Phys. C* **221**, 1 (1994)
46. Athe, P., Srivastava, S.: Tunable Fano resonance in one dimensional superconducting photonic crystal. *J. Supercond. Nov. Magn.* **28**, 2331–2336 (2015)